Proceedings Paper:
Abdullah, A., Jayachandran, J.T., Xie, S. Q. et al. (1 more author) (2024) Instantaneous Center of Rotation Trajectory Tracking of A Novel Five-bar Robotic Exoskeleton for Knee Rehabilitation. In: 2024 30th International Conference on Mechatronics and Machine Vision in Practice (M2VIP). 2024 30th International Conference on Mechatronics and Machine Vision in Practice (M2VIP), 03-05 Oct 2024, Leeds, United Kingdom. IEEE ISBN 979-8-3503-9192-3

https://doi.org/10.1109/M2VIP62491.2024.10745996

Instantaneous Center of Rotation Trajectory Tracking of A Novel Five-bar Robotic Exoskeleton for Knee Rehabilitation

1st :Ahmad Abdullah
School of Biomedical Sciences
University of Leeds
Leeds, UK
a.abdullah@leeds.ac.uk

2nd :Jaideep Thattamparambil Jayachandran
School of Biomedical Sciences
University of Leeds
Leeds, UK
J.ThattamparambilJayachandran@leeds.ac.uk

3rd :Sheng Quan Xie
Institute of Robotics and Autonomous Systems, School of Electronic and Electrical Engineering
University of Leeds
Leeds, UK
s.q.xie@leeds.ac.uk

4th :Aiqin Liu
School of Biomedical Sciences
University of Leeds
Leeds, UK
a.liu@leeds.ac.uk

***Abstract*—Knee Exoskeletons provide a way to restore the quality of life in people with knee disorders or after injury. One of the major limitations of these exoskeletons is to mimic the natural polycentric knee joint motion. The design and performance analysis of a novel five-bar mechanism is proposed in this study which can be used in a knee exoskeleton. The purpose of this study was to analyze the instantaneous center of rotation trajectory of the five-bar mechanism mimicking the natural knee center of rotation trajectory during sit to stand motion and compare it with similar existing mechanisms. The position analysis of the mechanism in a simplified configuration and the actual hardware configuration was performed for analyzing the center of rotation trajectory, both theoretically and using a dedicated tool respectively. The motion and the center of rotation trajectory of five-bar mechanism was validated, and the results of the study are presented which show the successful tracking of the reference Instantaneous center of rotation with an error as low as 0.14mm for the simplified configuration and 0.24mm for the actual configuration. These results were then compared with different bar mechanisms showing that our five-bar mechanism had better tracking performance among the available rigid mechanisms.**

Keywords—Instantaneous center of rotation (ICR), Five-bar Linkage Mechanism, Kinematics, Exoskeletons, Trajectory tracking

I. INTRODUCTION

Knee exoskeletons provide a solution for various knee related problems such as knee osteoarthritis and rehabilitation after surgery [1]. These wearable robots are specially designed to assist and facilitate the motion of the knee joint for various tasks such as walking, sit-stand, stair climbing and other related cyclic and non-cyclic activities [2, 3]. There are various types of lower limb exoskeleton such as cable driven exoskeletons [4], direct motor (rotary) driven exoskeletons, linear actuator driven exoskeletons [5] and specialized actuator driven exoskeletons [6, 7]. However, there are limitations associated with the design of these robots, foremost among which is the compliance of the exoskeleton with the natural motion of the human knee [8]. The compliance assures the safety, comfort and efficiency of the exoskeleton during use. A major factor affecting these parameters is the issue of multi-center or polycentric motion of the human knee joint, which originates from the complex anatomy of the knee joint. The motion of the knee joint is a combination of rolling and sliding actions at the articulation surfaces of the femur and tibia [9-11] .

The effectiveness of these assistive mechanisms lies in alleviating pain and discomfort by providing assistance as required [12]. It has been well established from past studies that motion of knee joint is polycentric and that the Instantaneous Centre of Rotation (ICR) follows a specific trajectory [13]. This trajectory may depend upon various factors such as BMI and limb lengths based on height of the patient. This polycentric motion poses a significant challenge for the exoskeletons designed to assist with knee joint movement.

To address this challenge, it is crucial to consider the knee joint's motion during flexion or extension in the sagittal plane, which is essential for locomotion and ambulation. The exoskeleton's mechanism must mimic this natural motion to prevent misalignment. Proper alignment will help avoid the excessive forces and torques that can build up at the joint, ensuring the exoskeleton operates safely and efficiently.

One of the most studied mechanism which mimics the actual ligament linkage in the knee is the four-bar mechanism [14-17].The mechanism presented in [14] was very bulky and weighs 3.5 kg. Additionally, while the study focused on providing the required torque, it did not address the issue of misalignment in detail. In [15], the four-bar has been used in

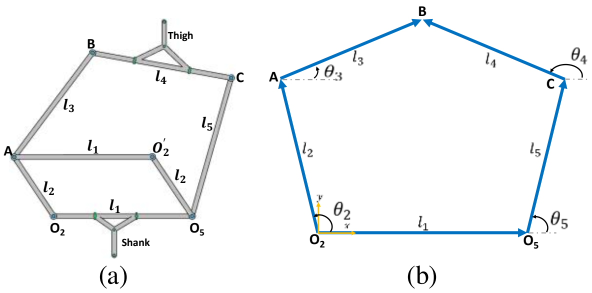

Fig. 1 The simplified schematics diagram of the five-bar mechasnism, (a) The coupling of the links, (b) The simplified arrangement of linkages

This research was funded under UKRI Impact Acceleration Account (IAA), University of Leeds, Faculty of Biological Sciences Impact & Innovation Award and UKRI Healthy Ageing Catalyst Award (ES/W006499/1).

lever-like configuration to support a load of up to an 85 kg person. The exoskeleton was intended to aid the workers in industry but featured a hinge-like joint that did not imitate the polycentric motion of a knee. An exoskeleton incorporating a four-bar mechanism, to follow the ICR, and a magnetorheological clutch to improve the torque transmission and compliance was presented in [16]. Despite its complex design, the ICR tracking error was still close to 3mm. A specialized knee joint design utilizing a double four bar linkage was presented in [17], where one four-bar linkage was used for ICR tracking and the second for force transmission. However, these designs face limitations, including complexity and higher error relative to the reference ICR. Alternatively, the literature has presented other specialized self-aligning mechanisms to address the misalignment problem. In [18], a 3-RRP parallel mechanism was employed to perform the required polycentric motion. The device could track any trajectory in space due to its parallel structure, but its limitations included a huge size, large weight, complexity, a 7.6% error in rotation and 1.7% error in translation. Another specialized mechanism employing Schmidt coupling to achieve polycentric motion was proposed in [19]. The authors studied the trajectory of both translation and rotation and recorded the effort of the patient using EMG as the quantitative measure of comfort. Although it was able to follow the ICR path, it had very low repeatability, resulting in a broad range of tracking error unsuitable for knee exoskeletons. A highly complex gears and cable-based hybrid mechanism was proposed in [20], reporting a significant average error of 2.52 mm in tracking the reference knee ICR trajectory. The complexity of the mechanism also limited its implementation as a wearable exoskeleton. An alternative approach was found in literature used joint angles in different activities like stand-to-sit (STS) and walking. The exoskeleton was designed to mimic the profile of the angles during STS and gait [21].

To overcome the above limitations, we previously designed a novel five-bar mechanism [22] to ensure the mimicking of the polycentric motion of the knee. The previous study showed the theoretical calculation of the ICR, and its tracking results as compared to the reference ICR. Building on this foundation, the current study aimed to evaluate the performance of the five-bar mechanism and develop a working prototype. The kinematics of the mechanism and the analysis of the ICR trajectory in its actual configuration is presented in section II and III. A detailed comparison between the reference ICR, results from different studies based on ICR trajectory tracking and the five-bar mechanism ICR trajectory tracking are presented in Section III and the hardware implementation is presented in Section IV. The conclusion is provided in Section V.

II. Method

A. *Kinematics*

The schematic diagram of five-bar mechanism is shown in Fig. 1. The line O_2O_5 formulates link 1 and is attached to the shank portion of the brace whereas the line joining BC forms link 4 which is attached to the thigh portion of the brace. The shank portion is considered ground for the purpose of this analysis. The link O_2O_5, O_2A, AB, BC, CO_5 all combine to form the five-bar mechanism. The lengths of the links are denoted by l_i and the corresponding angles are denoted by θ_i where $i = 1,2,\dots,5$. From the Fig. 1 (a), it is evident that the links $O_2'O_5$ and CO_5 are rigidly attached therefore the links O_2A and CO_5 have the same rotational velocity. The coupling of the mechanism due to the parallelogram formed by the links O_2O_5, O_2A, AO_2' and $O_2'O_5$ ensures that that the kinematic chain O_2ABCO_5 is in fact equivalent to a geared five-bar mechanism having gear ratio equal to 1. Since we required the position analysis to find the rotation of the output link, the vector closure method was employed to solve for these angles. The closed loop chain O_2ABCO_5 can be written as (1) as evident from Fig. 1 (b). This section utilizes the same mathematical relations formulated in the previous study [22].

$$\overrightarrow{O_2A} + \overrightarrow{AB} - \overrightarrow{O_2O_5} - \overrightarrow{O_2C} - \overrightarrow{CB} = 0 \tag{1}$$

The angles θ_3 and θ_4 can be given as (2) and (3).

$$\theta_3 = 2\left(atan2\left(-e_1 - \sqrt{e_1^2 + e_2^2 - e_3^2}, e_3 - e_2 \right), e_3 - e_2 \right) \tag{2}$$

$$\theta_4 = atan2\begin{pmatrix} -l_1 sin\theta_1 + l_2 sin\theta_2 + l_3 sin\theta_3 - l_5 sin\theta_5, \\ -l_1 cos\theta_1 + l_2 cos\theta_2 + l_3 cos\theta_3 - l_5 cos\theta_5 \end{pmatrix} \tag{3}$$

where

$$e_1 = -2l_3(l_1 sin\theta_1 - l_2 sin\theta_2 + l_5 sin\theta_5) \tag{4}$$

$$e_1 = -2l_3(l_1 cos\theta_1 - l_2 cos\theta_2 + l_5 cos\theta_5) \tag{5}$$

$$e_1 = l_1^2 + l_2^2 + l_3^2 - l_4^2 + l_5^2 - 2l_1l_2\cos(\theta_1 - \theta_2) + 2l_1l_5\cos(\theta_1 - \theta_5) - 2l_2l_5\cos(\theta_2 - \theta_5) \tag{6}$$

The link O_2A is considered as the input link in this analysis and the corresponding angle θ_2 is known as the input angle. The link 4, which is the thigh portion formed by the line BC, is considered as the output link and the corresponding angle θ_4 is known as the output angle. To mark the starting position in comparison to the knee joint, θ_2 and θ_5 are required to be specified as the initial angles of the mechanism. As the angle θ_2 changes, θ_4 also changes and therefore the mechanism can move between the extended and flexed positions. The initial angles and the lengths of mechanism were determined to correctly align the mechanism and mimic the natural polycentric motion of the human knee.

In addition to the link lengths and initial angles, another critical part in the position analysis of this five-bar mechanism is the location of ICR as the ICR trajectory is the key parameter in evaluating the performance of the mechanism. The ICR was calculated based on flexion and extension motion during sit to stand activity. Since link 4 is the output link, therefore the coordinates of point C are particularly important for the determination of the coordinates of the ICR of the mechanism. The angular velocity vector method was utilized to formulate the equation for the ICR for the five-bar mechanism. The coordinates of the ICR (I_{14x}, I_{14y}), are given by (7) and (C_x, C_y) are the coordinates for positions of point C both measured in O_2xy frame [22]. The ICR calculated using (7) is denoted as the theoretical ICR in this study.

$$\begin{bmatrix} I_{14x} \\ I_{14y} \end{bmatrix} = \begin{bmatrix} C_x + \dfrac{nl_4l_5\sin(\theta_3 - \theta_4)\cos(\theta_5)}{l_2\sin(\theta_2 - \theta_3) + nl_5\sin(\theta_3 - \theta_5)} \\ C_y + \dfrac{nl_4l_5\sin(\theta_3 - \theta_4)\sin(\theta_5)}{l_2\sin(\theta_2 - \theta_3) + nl_5\sin(\theta_3 - \theta_5)} \end{bmatrix} \tag{7}$$

For the purpose of verification and comparison of the position analysis and the ICR, the mechanism was analysed using an analysis tool named GIM which is a Graphical User Interface (GUI) based dedicated tool for the study of the mechanisms and kinematic chains [23]. The Mechanism was

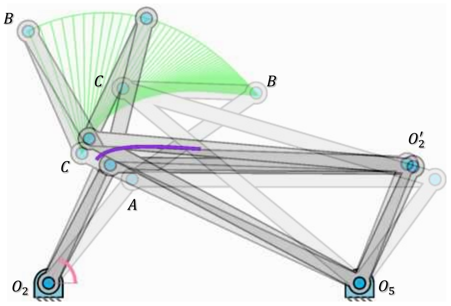

Fig. 2 The trajectory of instantaneous center of rotation of the Five-bar mechanism in its actual configuration

drawn to the scale using optimized link configuration and lengths. The points O_2 and O_5 act as the grounds and the link formed by joining the points $O_5O_2'C$ is a single rigid link. The input was applied at link 2 and the position analysis of the mechanism was performed. The range of motion of the mechanism and the corresponding trajectory of the ICR is shown in Fig. 2. The green shaded region shows the motion of the output link, link 4, when it was subjected to the input angle θ_2. The purple curve shows the changing ICR, indicating that the ICR experienced both translation and rotation as the flexion angle changed from 0º to 120º. The coordinates of the ICR were acquired from GIM Software. This ICR trajectory is denoted as the actual ICR trajectory in this study. The motion of link 4 depicted the position of the thigh portion of the leg moving from a fully extended position to a fully flexed position. The link configuration was based on the optimization study [22] which provided the optimized link lengths and calculated the optimal initial angles for the five-bar mechanism to follow the reference human knee ICR. The optimizing algorithms utilized the mechanism position analysis, constraints on lengths in terms of aesthetics and applicability and the ICR consideration to generate a vector containing the optimized links lengths and initial angles for the configuration. In the configuration shown in Fig. 2, the additional linkage between AO_2' provided the required coupling in the mechanism and did not affect the motion of the rest of links keeping the rest of the five-bar mechanism unchanged.

B. Knee reference ICR

For the reference knee ICR, the motion parameters from study [22] were utilized. The maximum range of flexion angle was considered to be 0 to 120 degree and the equation for the reference knee ICR can be given as (8). V, I, T_{PD} and T_{AP} denote knee varus rotation, internal rotation, proximal-distal translation, and anterior-posterior translation as a function of flexion angle β respectively [24]. Since the exoskeleton operates in the lateral sagittal plane, the ICR was plotted considering the exoskeleton at a lateral distance $X_k = 60mm$, accounting for the maximum medio-lateral width of the knee joint along with skin and orthosis spacing [25].

$$\begin{bmatrix} Y_k \\ Z_k \end{bmatrix} = \begin{bmatrix} -\sin(V) + T_{PD} \\ \cos(V)\sin(I)X_K + T_{AP} \end{bmatrix} \quad (8)$$

The equation for V, I, T_{PD} and T_{AP} can be given as (9) to (12).

$$V = 0.0791\beta - 5.733\times10^{-4}\beta^2 - 7.682\times10^{-6}\beta^3 + 5.759\times10^{-8}\beta^4 \quad (9)$$

$$I = 0.3695\beta - 2.958\times10^{-3}\beta^2 + 7.666\times10^{-6}\beta^3 \quad (10)$$

$$T_{PD} = -0.683\beta + 8.804E - 4\beta^2 - 3.750\times10^{-6}\beta^3 \quad (11)$$

$$T_{AP} = -0.1283\beta + 4.796\times10^{-4}\beta^2 \quad (12)$$

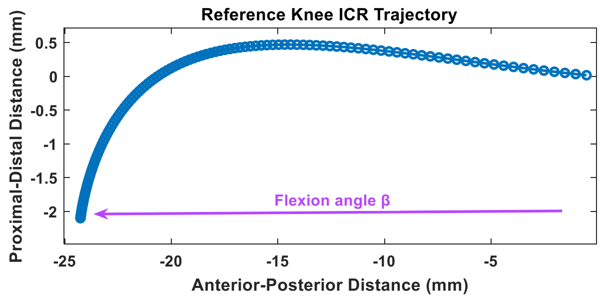

Fig. 3 The natural knee instantaneous center of rotation trajectory

The plot for the reference knee ICR calculated using (8) to (12) shows the trajectory of the knee ICR as the flexion angle changes from 0 to 120 degree (Fig. 3). Starting from a standing position, the translational motion is more dominant in the ICR trajectory. However, As the angle increases the rotational motion becomes more dominant closer to the sitting position. The average error between the reference ICR trajectory and the five-bar mechanism ICR trajectory was calculated using (13). This error was then compared to the error values reported in various studies (discussed in section III) to evaluate the performance of the mechanisms.

$$\frac{1}{n}\sum_{i}^{n}(E_i) \quad (13)$$

$$E_i = \sqrt{\left(Y_{K_{ref_i}} - Y_{mech_i}\right)^2 + \left(Z_{K_{ref_i}} - Z_{mech_i}\right)^2} \quad (14)$$

Where $i = 1,2,3..n$ denote the number of samples and Y_K, Z_K, Y_K and Z_K denote the respective coordinates for reference ICR and the mechanism ICR.

C. CAD modeling

The mechanism is actuated using the link 2 as the input link. Any rotation applied to the link 2 will result in rotation of the mechanism. The 3D model for the five-bar mechanism is given in Fig. 4. The CAD model is developed based on the actual configuration and the five-bar mechanism is fabricated based on this CAD model.

III. Results and Discussion

From the position analysis of the five bar mechanism, both in theory and using the hardware configuration in GIM as shown in Fig. 1 -Fig. 3, it is evident that the mechanism is in fact following a polycentric motion. The comparison of the actual knee ICR acquired using the analysis of the five-bar mechanism in GIM software against the reference knee ICR, given by (8), is shown in Fig. 5. As the flexion angle β was changed from 0 to 120, the actual (mechanism) ICR followed the trajectory of the reference ICR. Both the mechanism ICR and the reference ICR followed a translational path in the start.

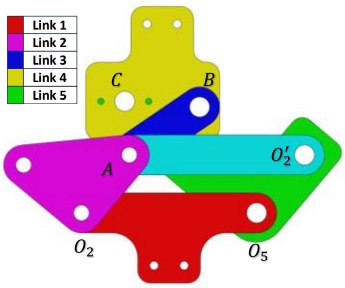

Fig. 4 The CAD model of Five-Bar mechanism configuration

This was referred to as the anterior-posterior translation. The change in centre of rotation of the knee was due to the motion of the human knee being a combination of rolling and sliding of femur over tibia. The average error between the reference ICR trajectory and both the theoretical ICR as well as the actual ICR trajectories was calculated for the complete range of motion. During initial phase of the flexion, there was more sliding motion which caused the translation of the femur with respect to tibia. In the later phase when femur was in place, due to Anterior Cruciate Ligament (ACL) and Posterior Cruciate Ligament (PCL), the rotation was more dominant and there was less translation. The rotation of the femur in relation to tibia gave rise to the bending of the knee hence the flexion is possible (Fig. 5).

TABLE 1 COMPARISON OF TRACIING ERROR FOR VARIOUS MECHANISM WITH THE PROPOSED MECHANISM

Exoskeleton	*Error value (mm)*	*Mechanism*
Five-bar (Proposed design)	0.24	Five-bar (actual)
MRKnee Exoskeleton [16]	3	Four-bar coupled with Clutch
Bioinspired Exoskeleton [20]	2.52±1.62	Rolling Joint & cable driven transmission
Knee joint for knee-ankle-foot orthosis [25]	0.2	Four-bar (Theoretical Only)
Knee kinematics compatible joint [26]	1.99	Four-bar
Wearable Perturbator [27]	1.06	Four-bar coupled with wafer discs

TABLE 1 shows a detailed comparison of trajectory tracking performance of various mechanisms from literature. This comparison focused on the error between the mechanism ICR trajectory and the reference ICR trajectory, highlighting the performance of the five-bar mechanism relative to other designs. The average and maximum theoretical ICR tracking error for our proposed five-bar mechanism is 0.16mm and 0.43mm respectively, as reported in [22]. The present study showed that the average and maximum actual ICR tracking error for the proposed five-bar mechanism, calculated using GIM software, were 0.24mm and 0.37mm, respectively. Further comparison from TABLE 1 shows that the maximum theoretical ICR error for a four-bar mechanism was reported to be 1.06mm in [27] and to be 0.2mm (theoretical) in [25]. These values are still higher than both the theoretical and actual ICR error for the proposed five-bar mechanism. It can be safely deduced from the table that the proposed five-bar mechanism has the minimum error and therefore follows the reference knee ICR better compared to a variety of bar mechanisms.

This research focused on one of the aspects of the knee exoskeleton design which is to mimic the natural knee movement. Other aspects, such as the exoskeleton's ability to provide the required amount of torque and enhance the mechanical advantage to perform the desired motion are currently under investigation.

IV. Hardware Implementation

The hardware prototype of the exoskeleton was developed with five-bar mechanism at its core for polycentric motion. The five-bar mechanism was fabricated using the aluminium

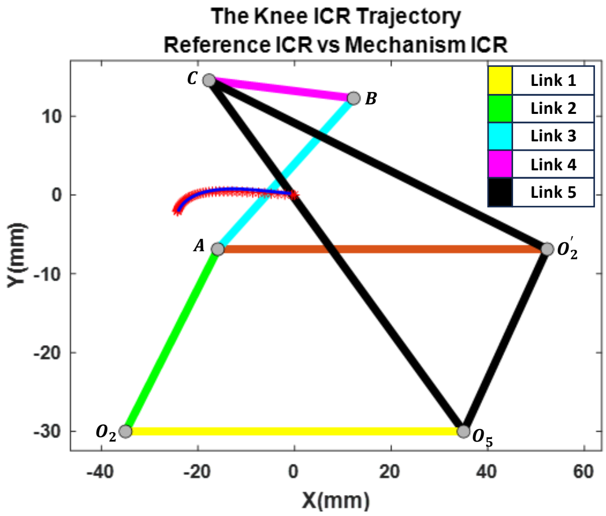

Fig. 5 The tracking performance of the Five-Bar mechanism: Five-bar ICR trajectory (blue) vs the reference knee ICR trajectory (red). X-axis is the anterior posterior motion and the proximal distal motion is on Y-axis.

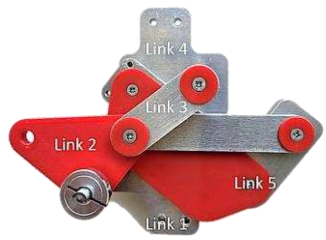

Fig. 6 The five-bar mechanism after fabrication

bars. The thigh and shank links were attached with aluminium bars which acted as the main structure of the exoskeleton. The bars had braces attached for support, which included straps for securing the thigh and shank of the wearer. The braces served as interface between the exoskeleton and the human, and they were padded to ensure the wearer's comfort during the operation.

The input link of the mechanism was considered as link 2 as the actuation from this link would ensure the desired polycentric motion. To move the mechanism between extension and flexion, a suitable range of motion of link 2 was considered, ensuring that the mechanism can cover the full range of flexion angle β (Fig. 3) which was chosen to be between 0 to 120 based on findings from literature in Section I. The coupling between the linkage allows for both translation and rotation of the whole mechanism ensuring polycentric motion. The flexion angle β was measured by placing a rotary encoder at the pin which was used to couple the links with the thigh plate (link 4). The rotation of this pin was the desired flexion angle output. The fabricated mechanism is shown in Fig. 6. The shape of the links was modified to keep it compact and light, but the dimensions of the links was the same as those from previous study for accurate tracking of the ICR.

V. Conclusion

This study presented a performance analysis for a proposed five-bar mechanism intended to be integrated with an exoskeleton to achieve natural human knee polycentric motion. The five-bar mechanism aimed to mitigate the misalignment between the knee joint and the exoskeleton, thereby avoiding undue loads on the knee joint in extension and flexion during sit to stand (STS) motion. The position analysis showed that the mechanism closely followed the ICR of the human knee, with a minor average error of 0.16mm in simplified form and 0.24mm in its actual configuration. Additionally, it demonstrated superior performance compared to various bar mechanisms, including the widely used four-bar mechanism, in following human knee motion. The hardware implementation of the five-bar mechanism validated the concept's applicability and compactness without compromising the ICR tracking performance and mechanical efficiency. Further improvement in the mechanism's tracking performance can be proposed based on the motion capture analysis of the mechanism during operation. Further studies will also address torque transmission and mechanical advantage enhancement to reduce the required torque.

Acknowledgment

This research was funded under UKRI Impact Acceleration Account (IAA), University of Leeds Faculty of Biological Sciences Impact & Innovation Award and UKRI Healthy Ageing Catalyst Award (ES/W006499/1). The authors are grateful to the funding agencies for their support.

References

[1] R. Wilmart, E. Garone, and B. Innocenti, "The use of robotics devices in knee rehabilitation; a critical review," *Muscles, Ligaments & Tendons Journal (MLTJ),* vol. 9, no. 1, 2019.

[2] Z. Wu, M. Yang, Y. Xia, and L. Wang, "Mechanical structural design and actuation technologies of powered knee exoskeletons: A review," *Applied Sciences,* vol. 13, no. 2, p. 1064, 2023.

[3] H. Aguilar-Sierra, W. Yu, S. Salazar, and R. Lopez, "Design and control of hybrid actuation lower limb exoskeleton," *Advances in Mechanical Engineering,* vol. 7, no. 6, p. 1687814015590988, 2015, doi: 10.1177/1687814015590988.

[4] S. Grosu *et al.*, "Driving Robotic Exoskeletons Using Cable-Based Transmissions: A Qualitative Analysis and Overview," *Applied Mechanics Reviews,* vol. 70, no. 6, 2018, doi: 10.1115/1.4042399.

[5] Z. Wang, Z. Zhou, L. Ruan, X. Duan, and Q. Wang, "Mechatronic Design and Control of a Rigid-Soft Hybrid Knee Exoskeleton for Gait Intervention," *IEEE/ASME Transactions on Mechatronics,* vol. 28, no. 5, pp. 2553-2564, 2023, doi: 10.1109/tmech.2023.3245810.

[6] C. B. Sanz-Morère *et al.*, "An active knee orthosis with a variable transmission ratio through a motorized dual clutch," *Mechatronics,* vol. 94, 2023, doi: 10.1016/j.mechatronics.2023.103018.

[7] J. Song, A. Zhu, Y. Tu, X. Zhang, and G. Cao, "Novel Design and Control of a Crank-Slider Series Elastic Actuated Knee Exoskeleton for Compliant Human–Robot Interaction," *IEEE/ASME Transactions on Mechatronics,* vol. 28, no. 1, pp. 531-542, 2023, doi: 10.1109/tmech.2022.3204921.

[8] M. d. C. Sanchez-Villamañan, J. Gonzalez-Vargas, D. Torricelli, J. C. Moreno, and J. L. Pons, "Compliant lower limb exoskeletons: a comprehensive review on mechanical design principles," *Journal of NeuroEngineering and Rehabilitation,* vol. 16, no. 1, p. 55, 2019/05/09 2019, doi: 10.1186/s12984-019-0517-9.

[9] G. Li, X. Liang, H. Lu, T. Su, and Z. G. Hou, "Development and Validation of a Self-Aligning Knee Exoskeleton With Hip Rotation Capability," *IEEE Transactions on Neural Systems and Rehabilitation Engineering,* vol. 32, pp. 472-481, 2024, doi: 10.1109/TNSRE.2024.3354806.

[10] J. D. Hassebrock, M. T. Gulbrandsen, W. L. Asprey, J. L. Makovicka, and A. Chhabra, "Knee Ligament Anatomy and Biomechanics," *Sports Medicine and Arthroscopy Review,* vol. 28, no. 3, pp. 80-86, 2020, doi: 10.1097/jsa.0000000000000279.

[11] M. Gao *et al.*, "Design and optimization of exoskeleton structure of lower limb knee joint based on cross four-bar linkage," *AIP Advances,* vol. 11, no. 6, 2021, doi: 10.1063/5.0053899.

[12] R. L. Medrano, E. J. Rouse, and G. C. Thomas, "Biological Joint Loading and Exoskeleton Design," *IEEE Transactions on Medical Robotics and Bionics,* vol. 3, no. 3, pp. 847-851, 2021, doi: 10.1109/TMRB.2021.3098920.

[13] Y. Wang, W. Zhang, D. Shi, and Y. Geng, "Design and Control of an Adaptive Knee Joint Exoskeleton Mechanism with Buffering Function," *Sensors (Basel),* vol. 21, no. 24, Dec 15 2021, doi: 10.3390/s21248390.

[14] J.-H. Kim *et al.*, "Design of a Knee Exoskeleton Using Foot Pressure and Knee Torque Sensors," *International Journal of Advanced Robotic Systems,* vol. 12, no. 8, p. 112, 2015, doi: 10.5772/60782.

[15] J. Noh, J. Kwon, W. Yang, Y. Oh, and J. H. Bae, "A 4-bar mechanism based for knee assist robotic exoskeleton using singular configuration," in *IECON 2016 - 42nd Annual Conference of the IEEE Industrial Electronics Society*, 23-26 Oct. 2016 2016, pp. 674-680, doi: 10.1109/IECON.2016.7793059.

[16] R. M. de Andrade, P. H. Fabriz Ulhoa, E. A. Fragoso Dias, A. B. Filho, and C. B. S. Vimieiro, "Design and testing a highly backdrivable and kinematic compatible magneto-rheological knee exoskeleton," *Journal of Intelligent Material Systems and Structures,* vol. 34, no. 6, pp. 653-663, 2022, doi: 10.1177/1045389x221117496.

[17] R. Barkataki, Z. Kalita, and S. Kirtania, "Anthropomorphic design and control of a polycentric knee exoskeleton for improved lower limb assistance," *Intelligent Service Robotics,* 2024/02/14 2024, doi: 10.1007/s11370-024-00512-x.

[18] M. A. Ergin and V. Patoglu, "A self-adjusting knee exoskeleton for robot-assisted treatment of knee injuries," in *2011 IEEE/RSJ International Conference on Intelligent Robots and Systems*, 25-30 Sept. 2011 2011, pp. 4917-4922, doi: 10.1109/IROS.2011.6095073.

[19] B. Celebi, M. Yalcin, and V. Patoglu, "AssistOn-Knee: A self-aligning knee exoskeleton," in *2013 IEEE/RSJ International Conference on Intelligent Robots and Systems*, 3-7 Nov. 2013 2013, pp. 996-1002, doi: 10.1109/IROS.2013.6696472.

[20] S. Yu *et al.*, "Bio-inspired design of a self-aligning, lightweight, and highly-compliant cable-driven knee exoskeleton," *Frontiers in Human Neuroscience,* vol. 16, p. 1018160, 2022, doi: 10.3389/fnhum.2022.1018160.

[21] S. V. Sarkisian, M. K. Ishmael, G. R. Hunt, and T. Lenzi, "Design, Development, and Validation of a Self-Aligning Mechanism for High-Torque Powered Knee Exoskeletons," *IEEE Transactions on Medical Robotics and Bionics,* vol. 2, no. 2, pp. 248-259, 2020, doi: 10.1109/TMRB.2020.2981951.

[22] A. Asker, S. Xie, and A. A. Dehghani-Sanij, "Multi-objective optimization of Force Transmission Quality and Joint Misalignment of a 5-Bar Knee Exoskeleton," in *2021 IEEE/ASME International Conference on Advanced Intelligent Mechatronics (AIM)*, 12-16 July 2021 2021, pp. 122-127, doi: 10.1109/AIM46487.2021.9517444.

[23] V. Petuya, E. Macho, O. Altuzarra, C. Pinto, and A. Hernandez, "Educational software tools for the kinematic analysis of mechanisms," *Computer Applications in Engineering Education,* vol. 22, no. 1, pp. 72-86, 2014, doi: https://doi.org/10.1002/cae.20532.

[24] P. S. Walker, J. S. Rovick, and D. D. Robertson, "The effects of knee brace hinge design and placement on joint mechanics," *Journal of Biomechanics,* vol. 21, no. 11, pp. 965-974, 1988/01/01/ 1988, doi: https://doi.org/10.1016/0021-9290(88)90135-2.

[25] G. M. Bapat and S. Sujatha, "A Method for Optimal Synthesis of a Biomimetic Four-Bar Linkage Knee Joint for a Knee-Ankle-Foot Orthosis," *Journal of Biomimetics, Biomaterials and Biomedical Engineering,* vol. 32, pp. 20-28, 2017, doi: 10.4028/www.scientific.net/JBBBE.32.20.

[26] J. M. B. Bertomeu *et al.*, "Development of a hinge compatible with the kinematics of the knee joint," *Prosthetics and Orthotics International,* vol. 31, no. 4, 2007. [Online]. Available: https://journals.lww.com/poijournal/fulltext/2007/31040/development_of_a_hinge_compatible_with_the.6.aspx.

[27] M. R. Tucker, A. Moser, O. Lambercy, J. Sulzer, and R. Gassert, "Design of a wearable perturbator for human knee impedance estimation during gait," in *2013 IEEE 13th International Conference on Rehabilitation Robotics (ICORR)*, 24-26 June 2013 2013, pp. 1-6, doi: 10.1109/ICORR.2013.6650372.